FEM-BEM ANALYSIS OF RADIO FREQUENCY DRYING OF A MOVING WOODEN PIECE

TEODOR LEUCA[1], MARCELA LAZA[1], LIVIA BANDICI[1], GABRIEL CHEREGI[1], GEORGE MARIAN VASILESCU[2], OANA MIHAELA DROSU[2]

Key words: Hybrid finite element method (FEM), Boundary element method (BEM), Drying in radiofrequency (RF) electromagnetic field, Wood industry.

The electric field has been computed using the hybrid technique FEM-BEM, so the motion modifies only the boundary conditions on the surface of the wooden piece; FEM mesh inside the piece as well as some of the elements of the matrix associated to the inner nodes remain unchanged. The electric field problem is coupled with the thermal field problem because the complex permittivity depends on the temperature and the specific losses are influenced by the electric field strength. Besides that, the moisturized wood to be dried is moving and the water vaporization has impact on the thermal field. Our paper proposes a method for solving the electric field problem coupled with thermal diffusion and mass problems, taking into consideration the movement of the wood object exposed to the drying process.

1. INTRODUCTION

The electric field inside the drying oven is produced by a set of electrodes powered by high voltages (8…20 kV) and frequencies of: 13.56, 27.12 and 40.66 MHz. The heating of the objects by radio frequency electromagnetic field produces a volume distribution of the specific losses that leads to a uniformly enough level of distributed thermal field inside the moisturized piece to be dried. The wavelength (> 10 m) is greater than the oven dimensions; there are not ferromagnetic parts, thus the derivative of magnetic flux density from Faraday's law can be neglected. A quasi-electrostatic problem has to be solved, where the electric permittivity is a complex quantity that depends on the temperature, therefore the electric field problem is coupled with the thermal diffusion one. The specific losses in the thermal diffusion equation depend on the electric field strength and the complex permittivity. The motion of the wet wood changes the geometrical structure needed for solving the electric field problem. Therefore the

[1] University of Oradea, Faculty of Electrical Engineering and Information Technology, 410087, Oradea, Romania; tleuca@uoradea.ro

[2] "Politehnica" University of Bucharest, 313 Splaiul Independenței, 060042 Bucharest, Romania

hybrid technique FEM-BEM is recommended for the computation of the electric field. This method presents the main advantages of the FEM [1–3]. The solution of the electric field problem coupled with the thermal and the mass ones for a 2D structure was presented in [4].

Our paper offers an analyzing procedure of the drying process for three-dimensional pieces of wood [5]. The integral equation on the 3D boundaries of the piece and of the electrodes defines the rigidity matrix that is the boundary condition for the electric field problem analyzed with FEM inside the piece.

The mathematical model of water vaporization is particularly complicated if we consider the diffusion of the water and the vapors within the volume of the wood related to its fibrous irregular structure. Moreover, this structure depends on the piece to be dried and it cannot be generally known. Therefore, we may assume that there is only surface vaporization, and then the diffusion inside the wooden piece is very rapidly done. Besides, the vaporization inside the piece must be avoided since it may lead to unwanted cracks. Evaporation on the wood surface reduces the temperature and it is part of the boundary condition of the thermal field problem. The speed of the wooden piece inside the oven has to be determined, such that the imposed moisture level to be reached at the exit from the oven.

2. THE INTEGRAL EQUATION OF THE ELECTRICAL POTENTIAL ON THE AIR BOUNDARY

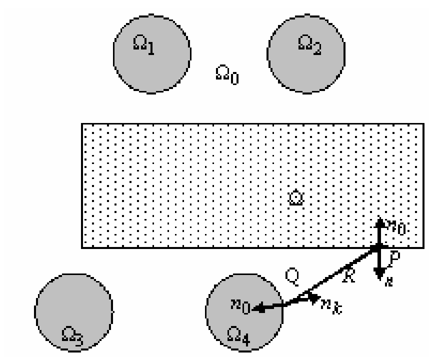

Fig.1 – Calculating domain.

On the boundary $\partial\Omega_0$ of the air domain Ω_0, consisting of the electrodes surfaces $\partial\Omega_k, k > 1$ and the boundary $\partial\Omega$ of the wood, the following integral equation for the electric potential and its normal derivative is valid [6]:

$$\theta V(P) = \int_{\partial\Omega} V \frac{\mathbf{R}\cdot\mathbf{n}}{R^3} \mathrm{d}S_Q - \int_{\partial\Omega} \frac{\partial V}{\partial n} \frac{1}{R} \mathrm{d}S_Q - \sum_k \int_{\partial\Omega_k} \frac{\partial V}{\partial n_k} \frac{1}{R} \mathrm{d}S_Q , \qquad (1)$$

where: θ is the solid angle under which a small vicinity of the domain Ω_0 is seen from the observation point P, $\boldsymbol{n}$ is the inner normal unit vector, at the integration point Q and $\mathrm{d}S_Q$ is the surface element in this point. If the observation point P is placed on $\partial\Omega_k$, then the left side of equation (1) becomes $4\pi V_k = 0$.

3. BEM DISCRETIZATION

We approximate the border $\partial\Omega_0$ with a polyhedral surface with triangular facets and admit that on each facet the derivative $\frac{\partial V}{\partial n}$ is constant, while V has a linear variation defined by the values of the potential from the nodes that border the triangle. Using nodal elements φ_j, the potential on the dielectric boundary $\partial\Omega$ is written as

$$V = \sum_{j=1}^{N} V_j \varphi_j \ , \tag{2}$$

where N is the number of nodes on $\partial\Omega$ boundary.

If we integrate equation (1) to the triangles on the surface of the dielectric, we obtain

$$A_{ss} V_s + B_{ss} \left(\frac{\partial V}{\partial n} \right)_s + B_{se} \left(\frac{\partial V}{\partial n} \right)_e = 0 \ , \tag{3}$$

where: V_s, $\left(\frac{\partial V}{\partial n} \right)_s$, $\left(\frac{\partial V}{\partial n} \right)_e$ are the matrices of potentials and derivatives after the normal on boundary $\partial\Omega$ and, respectively, of the derivatives after the normal on the boundary of electrodes $\partial\Omega_e = \bigcup_k \partial\Omega_k$. The elements of matrices A_{ss}, B_{ss} and B_{se} are determined by

$$a_{i,j}^{ss} = \frac{2\pi}{3} \chi_i(j) S_i - \int_{\Delta_i} \int_{\partial\Omega} \varphi_j(Q) \frac{\mathbf{R}(P,Q) \cdot \mathbf{n}}{R^3(P,Q)} \mathrm{d}S_Q \mathrm{d}S_P \ ,$$

$$i = 1,2,\ldots,\ N_b \ , \ j = 1,2,\ldots,\ N_n \tag{4}$$

$$b_{i,j}^{ss} = \int_{\Delta_i} \int_{\Delta_j} \frac{1}{R(P,Q)} \mathrm{d}S_Q \mathrm{d}S_P \ , \quad i,j = 1,2,\ldots,\ N_b \ , \tag{5}$$

$$b^{se}_{i,j_e} = \int\limits_{\Delta_i}\int\limits_{\Delta^e_j}\frac{1}{R(P,Q)}\mathrm{d}S_Q\mathrm{d}S_P\ ,i = 1,2,...,\ N_b \qquad \text{and} \quad j_e = 1,2,...,\ N^e_b\ , \tag{6}$$

where: Δ_i, Δ^e_j are triangles on $\partial\Omega$ and respectively $\partial\Omega_e$, $\chi_i(j)$=1 if node j borders triangle Δ_i and $\chi_i(j)$ = 0. Otherwise, S_i is the area of the triangle Δ_i, N_b and N_n are, respectively, the number of triangles and nodes on $\partial\Omega$, while N^e_b is the number of triangles on $\partial\Omega_e$. When we integrate equation (1) on the facets of the electrodes boundary, we obtain

$$A_{es}V_s + B_{es}\left(\frac{\partial V}{\partial n}\right)_s + B_{ee}\left(\frac{\partial V}{\partial n}\right)_e = C_e\ , \tag{7}$$

where the elements of matrices A_{es}, B_{es}, B_{ee} and C_e are determined by:

$$a^{es}_{i_e,j} = -\int\limits_{\Delta^e_i}\int\limits_{\partial\Omega}\varphi_j(Q)\frac{\mathbf{R}(P,Q)\cdot\mathbf{n}}{R^3(P,Q)}\mathrm{d}S_Q\mathrm{d}S_P\ ,\ i_e = 1,2,...,N^e_b,\ j = 1,2,...,N\ , \tag{8}$$

$$b^{es}_{i_e,j} = \int\limits_{\Delta^e_i}\int\limits_{\Delta_j}\frac{1}{R(P,Q)}\mathrm{d}S_Q\mathrm{d}S_P\ ,i_e = 1,2,...,\ N^e_b,\ \ j = 1,2,...,\ N_b\ , \tag{9}$$

$$b^{ee}_{i_e,j_e} = \int\limits_{\Delta^e_i}\int\limits_{\Delta^e_j}\frac{1}{R(P,Q)}\mathrm{d}S_Q\mathrm{d}S_P\ ,i_e = 1,2,...,\ N^e_b,\quad j_e = 1,2,...,\ N^e_b, \tag{10}$$

$$c_{i_e} = -4\pi\ S^e_i\ V_{i_e}\ . \tag{11}$$

Observations. i) If the wood moves, then only the values of the matrix coupling the electrodes and the wood B_{se} and the matrix of free terms C_e change.

ii) Matrices B_{ss} and B_{ee} are symmetric.

iii) $B_{se} = B^{\mathrm{T}}_{es}$, where T indicates the transpose. It is sufficient to determine only one of the two matrices. Calculation effort is substantially reduced in the case of structures with moving bodies, where these matrices are determined at each time step.

We multiply equation (7) with B^{-1}_{ee} and replace $\left(\frac{\partial V}{\partial n}\right)_e$ in equation (3). We obtain

$$D_sV_s + E_s\left(\frac{\partial V}{\partial n}\right)_s = F_s\ , \tag{12}$$

where

$$D_s = A_{ss} - B_{se} B_{ee}^{-1} A_{es} \ , \tag{13}$$

$$E_s = B_{ss} - B_{se} B_{ee}^{-1} B_{es} \ , \tag{14}$$

$$F_s = -B_{se} B_{ee}^{-1} C_e \ . \tag{15}$$

Equations (12) and (3) form a system of equations in which the unknown elements are the potentials of nodes V and the values of the derivates $\frac{\partial V}{\partial n}$ on the triangular facets of the dielectric.

4. **ELECTRIC FIELD PROBLEM INSIDE THE WOOD**

The solution of the sinusoidal electric field problem in the wood domain Ω (Fig.1) is obtained by using phasor representation. The complex permittivity of the wood is: $\underline{\varepsilon} = \varepsilon' - j\varepsilon''$. Since we can neglect the derivative of magnetic flux density in the Faraday law, the electric potential satisfies equation

$$\nabla \cdot \underline{\varepsilon} \nabla \underline{V} = 0 \ . \tag{16}$$

The boundary condition is given by the continuity of the normal component of the electric flux density

$$\underline{\varepsilon}_r \frac{\partial \underline{V}}{\partial n} = \frac{\partial V}{\partial n} \ . \tag{17}$$

5. **BEM DISCRETIZATION**

For the numerical solving of equation (16) we choose a tetrahedron network and the first order nodal elements:

$$\underline{V} = \sum_{n=1}^{N} \underline{\eta}_n \varphi_n \ . \tag{18}$$

Using Galerkin technique equation (16) and boundary condition (17), we have:

$$\int_{\Omega} \nabla\varphi \cdot \underline{\varepsilon} \nabla \underline{V} \mathrm{d}\Omega + \int_{\partial\Omega} \varphi \underline{\varepsilon} \frac{\partial V}{\partial n} \mathrm{d}S = 0 \ , \tag{19}$$

where φ is the node-shaped element of order 1. On the border we have a relationship between the potential *V* and its derivative by the normal $\frac{\partial V}{\partial n}$, given by equation (3) and (12) written on the boundary $\partial\Omega$.

6. THE THERMAL DIFFUSION PROBLEM, COUPLED WITH THE MASS PROBLEM AND MOTION OF THE WOODEN PIECE

The diffusion of the thermal field is described by the equation

$$-\nabla\lambda\nabla T + c\frac{\partial T}{\partial t} = p \;, \tag{20}$$

where λ is the thermal conductivity, *c* is the volume thermal capacity, and the specific losses in the dielectric are given by relation: $p = E^2\omega\varepsilon'\,\mathrm{tg}\delta$,where the electric field strength *E* is obtained from the electric field problem. The boundary condition is

$$-\lambda\left(\partial T/\partial n\right) = \alpha(T - T_e), \tag{21}$$

where: α is the coefficient of thermal transfer on the surface, and T_e is the temperature outside the piece of wood. The numerical solution of the equation (20) is given by FEM, using the same mesh as within the problem of electric field, while the time discretization has been done using the trapeze method.

The water vaporization from the wooden mass takes place in a small part inside the wooden piece and largely on its surface. To take into consideration the inner vaporization leads to the computation of a complicated water diffusion problem in which a non-homogeneous pressure field interferes due to the water vapors. The high anisotropy of the wood, due to the orientation of the wooden fibers, makes almost impossible the water diffusion problem to be accurately modeled. Additionally, for drying processes, the rapid appearance of water vapors from the inner part of the wood can lead to its destruction. For this reason, the maximum temperature inside the wooden object has to be limited (bellow 70^0C). Thus, we can neglect the inner vaporization and take into consideration only that one on the surface of the wood. The evaporation speed on the surface unit depends on the difference between the temperature on the surface of the wood and the ambient temperature. It also depends on the degree of saturation of the vapors, on the air pressure, on the air flow in the proximity of the wooden object etc.

We admit that the evaporation speed $\frac{\mathrm{d}\tau_s}{\mathrm{d}t}$ of the water on the unit surface linearly depends on temperature

$$\frac{d\tau_s}{dt} = w\left(T - T_e\right) . \tag{22}$$

If Λ is the latent heat of the vaporization volume, then the loss of the heat due to the vaporization on the surface reduces the temperature on the surface alike the thermal convection. So, we can take into consideration the vaporization by using a virtual convection coefficient in the boundary condition (6), according to the relation:

$$\alpha_{ech} = \alpha + \Lambda w . \tag{23}$$

The estimation of the temperature field on the interval $[t_i, t_{i+1}]$ allows the calculation of the water volume evaporated during this interval:

$$-(V_{water}^{i+1} - V_{water}^{i}) = \frac{1}{2} \oint_{\partial\Omega} w\left(T(t_{i+1}) + T(t_i)\right) \Delta t_i \mathrm{d}l . \tag{24}$$

This leads to a change of the piece moisture. The physical parameters of the wooden piece depend on temperature and moisture and they are iteratively rectified at each time step. The computation of the moving speed inside the oven requires the following procedure: the requisite time for reaching the imposed moisture value for the stationary piece is calculated; then the oven active length is divided by this time. Since the electric field depends on the position, the speed can be slightly reduced.

7. **RESULTS**

The drying appliance has 5 pairs of electrodes with a diameter of 10 mm and a length of 150 mm on the O*x*-axis, and the dielectric material has the sizes x = 80 mm, y = 100 mm and z = 10 mm (Fig. 2). The dielectric has the following properties: permittivity ε'= 6.5, loss factor tg δ = 0.1, thermal conductivity λ = 0.41 W/m$\cdot{}^0$C, water mass density τ = 1 000 kg/m^3, wood heat capacity c = 2 000 J/kg$\cdot{}^0$C, convection heat transfer coefficient α_c = 15 W/m^2 ^{0}C, frequency f = 13.56 MHz. The wood used in this situation has an initial moisture content of 45%, at the end of the drying process a value of 10% being obtained, when it is considered that the wood is dry. The mesh network has 1071 tetrahedral elements and 281 nodes.

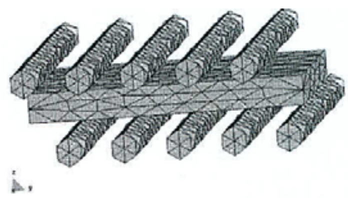

Fig. 2 – RF drying appliance.

If the piece of wood does not move we obtain the results in Figs. 3–5 for different operating voltages of the electrodes.

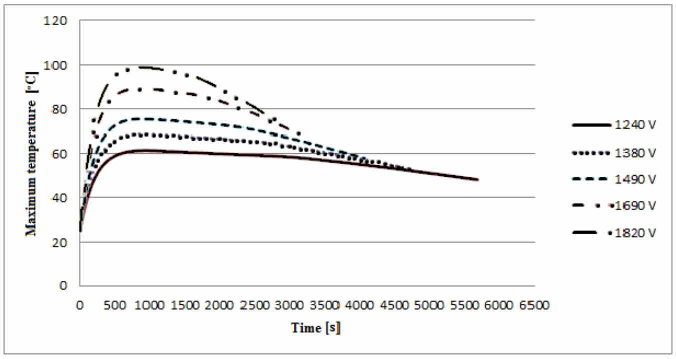

Fig. 3 – The maximum temperature calculated in the volume of the stationary dielectric in relation to time for different anode voltages.

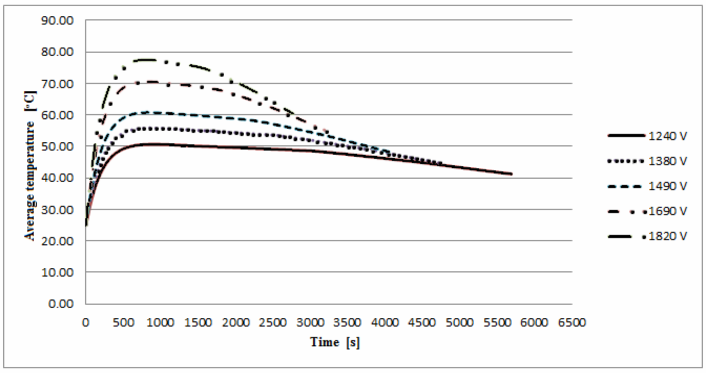

Fig. 4 – The average temperature calculated in the volume of the stationary dielectric in relation to time for different anode voltages.

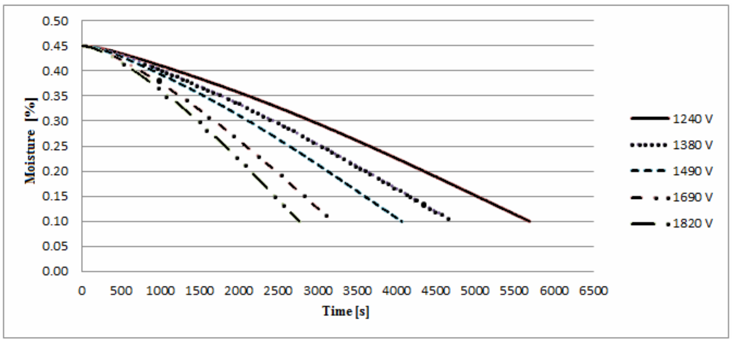

Fig. 5 – The variation of the moisture of the stationary dielectric in relation to time for different anode voltages.

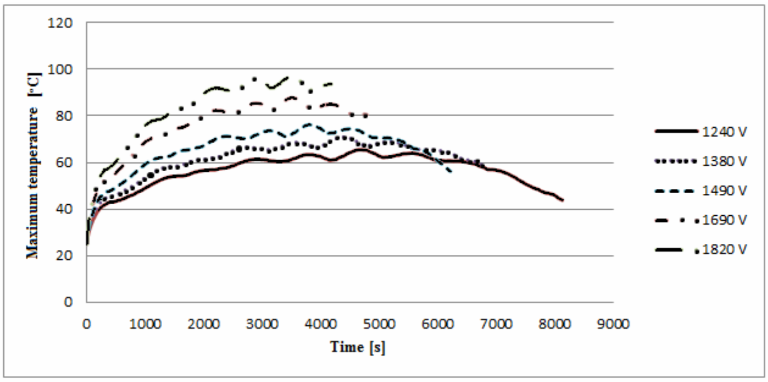

Fig. 6 – The maximum temperature calculated in the volume of the moving dielectric in relation to time for different anode voltages.

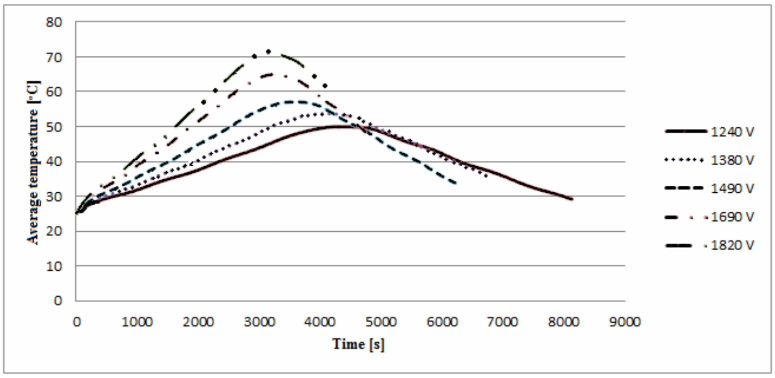

Fig. 7 – The average temperature calculated in the volume of the moving dielectric in relation to time for different anode voltages.

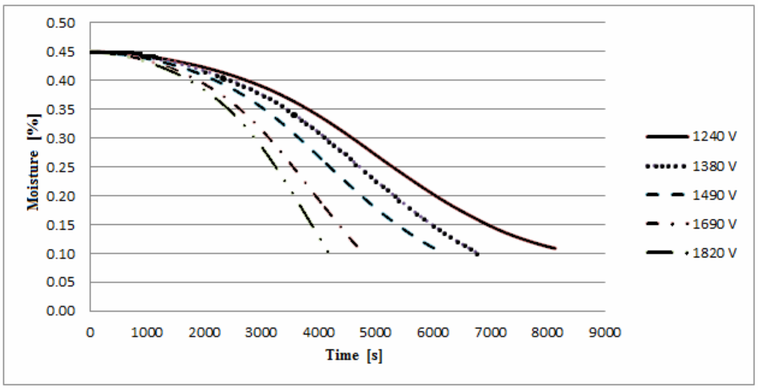

Fig. 8 – The variation of the moisture of the moving dielectric in relation to time for different anode voltages.

The speed by which the dielectric moves inside the applicator is determined automatically by the software after the first run in which it sets the time necessary for the drying of the dielectric when it is stationary, and placed in the center of the applicator. This value of the speed ensures that, when it exits the applicator, the dielectric is dry. If desired, speed may be changed and made variable over time.

If the piece of wood is moving we obtain the results in Figs. 6–8 for different operating voltages of the electrodes.

8. **CONCLUSIONS**

The hybrid FEM-BEM method developed in this paper for the analysis of the radiofrequency electromagnetic field used to dry moving dielectrics has the great advantage that the mesh network remains unchanged when the dielectric moves. Therefore, the FEM matrices used to discretize the electric field (19) and the thermal field (20) remain unchanged, being calculated once at the beginning of the movement. Also, some of the BEM matrices remain unchanged (the coupling matrices between their own surfaces). Only the coupling matrix between the surface of the wood and that of the electrodes is recalculated at each step of movement. For the evaporation of water we suggested a simple model, in which the evaporation is allowed to take place only at the surface of the wood, and the diffusion of water in the wooden mass is done instantly. The importance of the presented study consists in the fact that the maximum temperature, that cannot exceed 100^0C, can be estimated, and, for different electrode voltages, we can be recommended the moving speeds.

Received on June 30, 2014

REFERENCES

1. W. Trowbridge, *Computing electromagnetic field for research and industry: major achievements and future friends*, IEEE Trans. Magn., **32**, *3*, pp. 627–630, 1996.
2. M.A. Tsili, A.G. Kladas, P. S. Georgilakis, A.T. Souflaris, C.P. Pitsilis, J. A. Bakopoulos, and D. G. Paparigas, *Hybrid numerical techniques for power transformer modeling: a comparative analysis validated by measurements*, IEEE Trans. Magn., **40**, *2*, pp. 842–845, 2004.
3. M. Maricaru, *Integral methods for solving the electromagnetic filed problems* (in Romanian), PhD Thesis, UPB Bucharest, 2007.
4. T. Leuca, D. Spoiala, L. Bandici, *A method of solving the electromagnetic, thermal and mass problems, in the drying processes of wood in the RF field, IGTE Symposium*, September 17–20, 2006, Graz University of Technology, Austria, pp. 406–409.
5. M. I. Laza, *Contributions to the numerical modelling of dielectric processing in a high-frequency electromagnetic field. Computer-aided design elements of radio frequency and microwave equipment*, PhD Thesis, University of Oradea, 2013.
6. H. Gavrila, Fl. Hantila, M. Maricaru, M. Vasiliu, *Treatment of the multiply connected domains in numerical analysis of magnetic boundary value problems*, Rev. Roum. Sci. Techn. Electrotechn. et Energ., **48**, pp. 167–177, 2003.